Hydrodynamic Shape Genealogy for Teardrop-shaped Autonomous Underwater Vehicles

Tiantian Liu, Yuhong Liu*, Lianhong Zhang, Hongwei Zhang, Zhiliang Wu, Yanhui Wang
Key Laboratory of Mechanism Theory and Equipment Design of Ministry of Education,
School of Mechanical Engineering, Tianjin University
Tianjin 300072, China
* Corresponding author: yuhong_liu@tju.edu.cn

***Abstract*—More diverse marine tasks and longer range water missions require the hydrodynamic shape, viz. hull shape, of Autonomous Underwater Vehicles (AUVs) for both efficient design and least resistance. Therefore a systematic design for the hydrodynamic shape of AUVs is needed and necessary to meet the various requirements. In the present work, a hierarchical classification for the hull shape of AUVs was proposed according to the shape characteristics of the main hull of AUVs. Focused on the teardrop-shaped AUVs, hydrodynamic drags of a series of hull shapes were computed and analyzed using the computational fluid dynamics (CFD) simulation method with different hull shape parameters and Reynolds numbers (Re). The general mathematical model of volumetric coefficient of hydrodynamic drag and hull shape parameters, i.e., length diameter ratio (L/D), nose length diameter ratio (L_n/D), tail length diameter ratio (L_t/D) and Reynolds number (Re), was established and verified. The present work makes it possible to efficiently design the hull shape with minimum drag.**

Keywords—*autonomous underwater vehicles; hydrodynamic shape genealogy; volumetric coefficient model, efficient design*

I. Introduction

Autonomous Underwater Vehicles (AUVs) including the propeller-driven autonomous underwater vehicles and buoyancy-driven autonomous underwater gliders are widely used in marine observation and detection missions. Hydrodynamic shape of AUVs not only affects the structural assembly, pressure distribution and displacement of the internal structure, but also influences hydrodynamic performances, such as hydrodynamic force, noise, maneuverability and stability [1-4]. The design of AUVs requires the lowest energy consumption and noise as well as, the best stability and maneuverability, but some of these requirements are conflicting in nature. Generally, different tasks focus on different hydrodynamic requirements. Therefore, systematic design for the hydrodynamic shape of AUVs is desired to balance different requirements [5].

Many scholars have done a great deal of researches on hydrodynamic performance of AUVs and obtained substantial achievements. Yamamoto [6] changed the cylindrical shell into spindle hull to obtain a lower drag in the design of "Urashima" AUV for a longer cruising range. Nouri et al. [2] proposed a method for AUV hull design based on desired pressure distribution by adjusting the shape parameters. Alam et al. [7] proposed an optimization framework for the hull design of AUV to optimally design a torpedo-shaped AUV with an overall length of 1.3 m. In addition, Li [8] reviewed Studies on hydrodynamic characteristics of different hull shapes, such as drop-shape, low-drag shape and blended wing body. Most of the researches focused a particular design mission or object, and cannot be adapted to other design cases rapidly.

More diverse marine tasks and longer range missions require the hydrodynamic shape of AUVs both to realize rapid design and to have the least resistance. Therefore a systematic design for the hydrodynamic shape of AUVs is needed and necessary to meet the various requirements. In the present work, a hydrodynamic shape genealogy (HSG) of AUVs was proposed to meet rapid design of the AUVs with least hydrodynamic drag.

The genealogy in this paper does not trace the origin of the hull shape of AUVs, but provides a systematic classification method for rapid design of the hydrodynamic shape of AUVs. Study on the HSG of AUVs is to classify the hull shapes based on the relationship between characteristics of the hydrodynamic performance, and to discuss how the hydrodynamic drag changing with the hull shape parameters, finally to establish a mathematical model of genealogy of a given class of hull shapes.

The remainder of this paper is organized as follows. Hierarchical classification for the HSG of AUVs was presented in Section II. The hydrodynamic drag performance of AUVs with a teardrop-shaped hull was investigated and analyzed in Section III. In Section IV, the volumetric coefficient mathematical model was established and verified. The conclusions were given in the last section.

II. Hydrodynamic Shape Genealogy

In a broad sense, genealogy [9] means a system composed of things that have an inheritance relationship in historical development or a common law. In the present work, hierarchical classification was used to study on the HSG of AUVs. Hierarchical classification is a classification method based on the kinship and the basic nature of things. It can inform the hierarchical and affinity-disaffinity relationships among objects in a system [10].

According to the hydrodynamic performances of different cross-section shapes, hydrodynamic shapes of AUVs can be divided into three classes, including rotor, flat and irregular. Each class can be subdivided into different species according to the shape features in longitudinal cross-section, as shown in Fig. 1. For example, the species of Myring-shape belongs to the class of rotor. The hydrodynamic performance of the hull

978-1-5090-5278-3/17/$31.00 ©2017 IEEE

shape at the right end of genealogical tree can be discussed under different hull shape parameters and Reynolds numbers. Then, relationship between the hydrodynamic performance of each class in the genealogical tree and the hull shape parameters at the right end of the genealogical tree can be explored. The high-efficiency design of the hull shape of AUVs with optimal hydrodynamic drag can be achieved using this relationship.

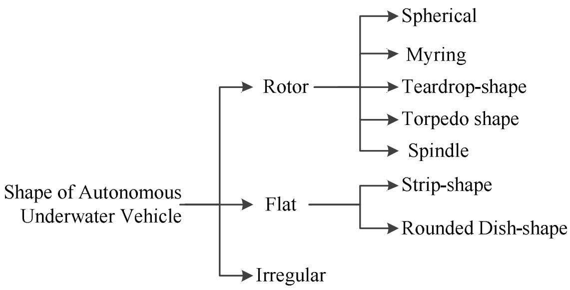

Fig.1. Genealogical tree of hydrodynamic shape of AUVs

III. CASE STUDY

AUVs are always expected to have the minimum drag, and the maximum cruising range and velocity. The teardrop-shape is widely applied to the hull shape of AUVs for its lower resistance and good assembly performance. So, in the present work, the species of Teardrop-shape in the class of rotor was used as the case to investigate the effects of Reynolds number and shape parameters on the drag coefficient. Figure 2 shows the geometric profile of teardrop-shape.

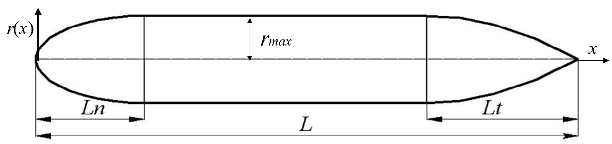

Fig.2. Parameterized shape of the Teardrop-shape

The parameterized shape of the teardrop-shaped body is given

$$r(x)=\begin{cases} r_{\max}\left(1-\left(\dfrac{L_n-x}{L_n}\right)^{n_n}\right)^{1/n_n} & for\,0\le x\le L_n \\ r_{\max} & for\,L_n\le x\le L-L_t \\ r_{\max}\left(1-\left(\dfrac{x-L+L_t}{L_t}\right)^{n_t}\right) & for\,L-L_t\le x\le L \end{cases} \tag{1}$$

where $r_{\max}$ is the maximum radius of the hull, L is the total length of the AUV, L_n and L_t are the lengths of the nose and the tail respectively, and n_n and n_t are shape indexes associated with the nose and tail shapes respectively. The profiles of nose and tail will go blunt with the increasing n_n and n_t.

Generally, the hydrodynamic drag (D) is the sum of the viscous drag D_{PV} and frictional drag D_{FV}. Those drags can be expressed by their non-dimensional drag coefficients [11]

$$C_{DV}=\frac{D}{\frac{1}{2}\rho v^2\nabla^{\frac{2}{3}}}=C_{PV}+C_{FV}=\frac{D_{PV}}{\frac{1}{2}\rho v^2\nabla^{\frac{2}{3}}}+\frac{D_{FV}}{\frac{1}{2}\rho v^2\nabla^{\frac{2}{3}}} \tag{2}$$

where C_{DV} is the volumetric coefficient of hydrodynamic drag, C_{PV} is the volumetric viscous pressure drag coefficient, C_{FV} is the volumetric frictional drag coefficient, v is the velocity of the vehicle, ρ is the density of the fluid, ρ=1020 kg/m^3, and ∇ is the volume of the vehicle (m^3).

Parameters of C_{PV}, C_{FV}, D_{PV} and D_{FV} were calculated by the computational fluid dynamics (CFD) simulation. The SST $k-\omega$ model was used in this paper to calculate the drag of AUV. Research showed that the SST $k-\omega$ model is accurate enough for the resistance prediction of AUVs [12]. The calculation domain is a cylinder with a diameter 50 times that of the AUV and a length 8 times that of the AUV, taking 3 units in front of the head as the water inlet, and 4 units behind the tail as the water outflow. The cylinder's flank is treated as symmetric and all the faces of the AUV are set as wall condition. The number of the total grids is about 3 million.

In the present work, the single variable method was used to analyze the effect of the shape indexes of nose and tail, Reynolds number and length diameter ratio on C_{PV}, C_{FV} and C_{DV}.

A. *Effect of Shape indexes on Drag Coefficients*

Figure 3 shows the changes of drag coefficients with the shape index n_n of the nose and the index n_t of the tail. From Fig. 3, all the three coefficients of C_{PV}, C_{FV} and C_{DV} change slightly with the increase of the shape indexes n_n and n_t. It is deemed that the n_n and n_t have little influence on the volumetric drag coefficients. Both n_n and n_t are set 2 in the subsequent calculation.

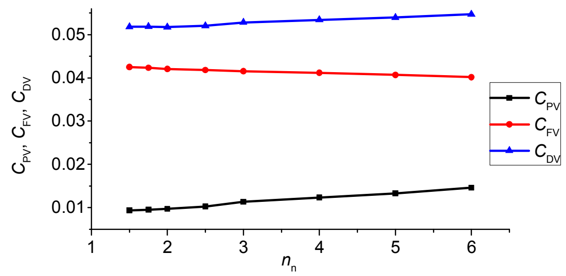

(a) Drag coefficients C_{PV}, C_{FV}, C_{DV} vs. n_n.

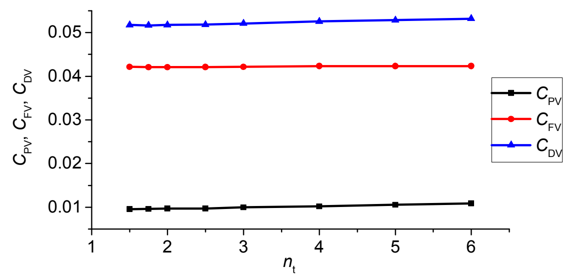

(b) Drag coefficients C_{PV}, C_{FV}, C_{DV} vs. n_t.

Fig.3. Drag coefficients at different shape indexes n_n and n_t of the nose and tail (Re=1.525×10^6, L/D=8, L=3 m, v=0.5 m/s, L_n/D=1.5, L_t/D=2)

B. *Effect of Length Diameter Ratio on Drag Coefficients*

The length diameter ratio (L/D) has a maturing effect on the hydrodynamic drag of AUVs. In the present work, values of L/D were chosen from 4 to 12. Figure 4 presents the influences of the parameter L/D on the drag coefficients C_{FV} and C_{PV}. From Fig. 4, the pressure drag coefficient C_{PV} decreases while increasing the L/D with the behavior of inverse function. The frictional drag coefficient C_{FV} increases linearly with increasing the L/D.

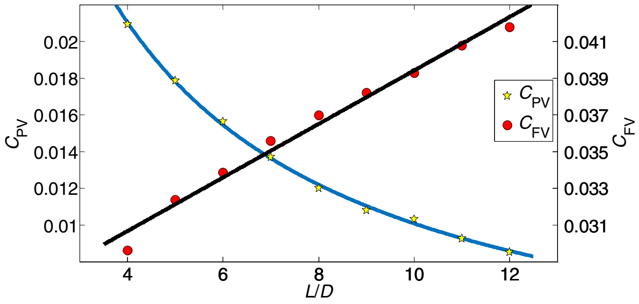

Fig.4. Drag coefficient at different length diameter ratios (Re=1.525×10^6, L=3 m, v=0.5 m/s, L_n/D=1.5, L_t/D=2, n_n=2, n_t=2)

C. *Effect of Reynolds Number on Drag Coefficients*

Reynolds number (Re) is mainly determined by characteristic length and cruising speed of the AUV. It gives $\mathrm{Re}=\dfrac{\rho v L}{\mu}$, where ρ is the water density, v is the velocity of the AUV, L is the characteristic length of the AUV, and μ is dynamic viscosity of water. To middle and small AUVs, the Re ranges between 10^6 and 10^7, and to gliders, the Re ranges between 3×10^5 and 10^6 [3]. So, range of Re from 1.58×10^5 to 1.58×10^7 was considered in the present work.

The drag coefficients of C_{PV} and C_{FV} are illustrated in Fig. 5. It is obvious that the drag coefficient decreases with Re in the selected range. When the Re is smaller than 2×10^6, C_{PV} declines sharply with the increase of Re. From Fig. 5, the relationship between C_{PV} and lgRe can be expressed by a three order polynomial, and the relationship between C_{FV} and lgRe can be described with Rational function.

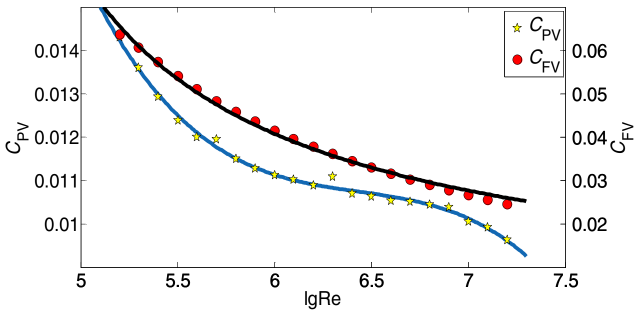

Fig.5. Drag coefficients at different Reynolds numbers (L/D=9 m, L=3 m, L_n/D=1.5, L_t/D=2, n_n=2, n_t=2)

IV. METHEMATICAL MODEL OF DRAG COEFFICIENT

According to the potential shapes of the teardrop-shaped AUVs, values of the shape parameters and Re used in the present case are decided and listed in Table I.

TABLE I. THE PARAMETERS OF AUV

Shape parameter	***reasonable ranges***
L/D	[4, 12]
L_n/D	[0.75, 2]
L_t/D	[1, 2.25]
n_n	2
n_t	2
Re	[1.58×10^5,1.58×10^7]

A. *Volumetric Viscous Pressure Drag coefficient*

According to Fig. 4, the relationship between C_{PV} and L/D can be expressed as

$$C_{PV}=\frac{p}{\dfrac{L}{D}+q} \tag{3}$$

where p and q are undetermined parameters related to the length diameter ratio (L_n/D) of the nose and length diameter ratio (L_t/D) of the tail. That is to say, p and q vary with L_n/D or L_t/D.

Figure 6 shows the values of p_n, q_n, p_t and q_t at different L_n/D and L_t/D, respectively. The subscripts n and t identify that the parameters p and q are related to the nose and tail, respectively.

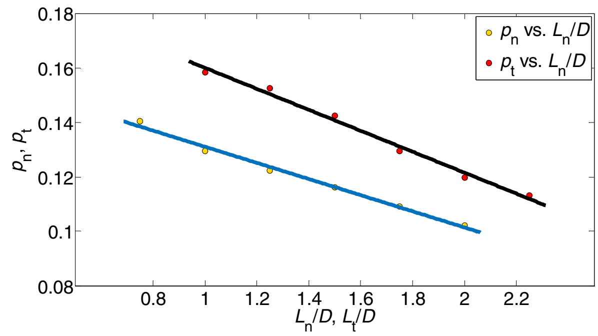

(a) p_n, p_t vs. L_n/D, L_t/D

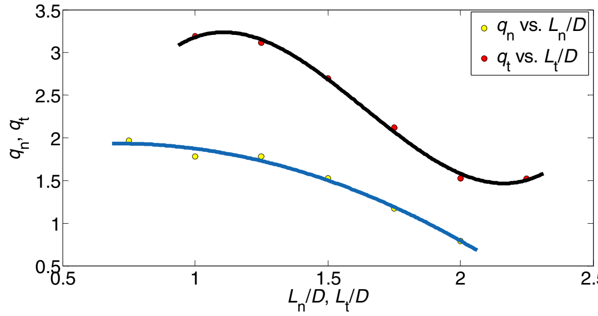

(b) q_n, q_t vs. L_n/D, L_t/D

Fig.6. The values of p, q with different L_n/D and L_t/D (Re=1.525×10^6, L=3 m, v=0.5 m/s, n_n=2, n_t=2)

According to Figs. 6, p_n and q_n go down with increasing the L_n/D and L_t/D linearly, respectively. The relationship between q_n and Ln/D, and that between q_t and L_t/D follow quadratic function and cubic function, respectively. They are

$$p_n = -0.02963\frac{L_n}{D} + 0.1507 \tag{4}$$

$$p_t = -0.04001\frac{L_t}{D} + 0.1999 \tag{5}$$

$$q_n = -0.6744\left(\frac{L_n}{D}\right)^2 + 0.9442\frac{L_n}{D} + 1.604 \tag{6}$$

$$q_t = 3.01\left(\frac{L_t}{D}\right)^3 - 14.77\left(\frac{L_t}{D}\right)^2 + 21.65\frac{L_t}{D} - 6.71 \tag{7}$$

Substituting (4)-(7) into (3) results in

$$C_{PV} = \frac{-0.02963\frac{L_n}{D} - 0.04001\frac{L_t}{D} + 0.2425075}{\frac{L}{D} - 0.67\left(\frac{L_n}{D}\right)^2 + 0.94\frac{L_n}{D} + 3.01\left(\frac{L_t}{D}\right)^3 - 14.77\left(\frac{L_t}{D}\right)^2 + 21.65\frac{L_t}{D} - 6.66} \tag{8}$$

From Fig. 5, relationship between C_{PV} and Re can be

$$C_{PV} = p_1(\lg \mathrm{Re})^3 + p_2(\lg \mathrm{Re})^2 + p_3(\lg \mathrm{Re}) + p_4 \tag{9}$$

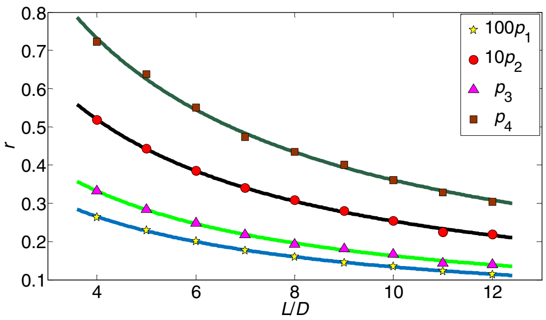

Fig.7. The value of p_1, p_2, p_3, p_4 with different L/D (L=3 m, L_n/D=1.5, L_t/D=2, n_n=2, n_t=2)

where p_1, p_2, p_3, p_4 are undetermined parameters related to the length diameter ratio (L/D).

Figure.7 shows the values of p_1, p_2, p_3, p_4 under different L/D. From Fig. 7, parameters of p_1, p_2, p_3, p_4 all decrease with increasing the L/D following rational function, and can be expressed as

$$p_1 = \frac{-0.01564}{\frac{L}{D} + 1.654} \tag{10}$$

$$p_2 = \frac{0.02961}{\frac{L}{D} + 1.702} \tag{11}$$

$$p_3 = \frac{1.906}{\frac{L}{D} + 1.743} \tag{12}$$

$$p_4 = \frac{4.282}{\frac{L}{D} + 1.824} \tag{13}$$

Substituting (10)-(13) into (9) results in

$$C_{PV} = \frac{-0.01564(\lg\mathrm{Re})^3 + 0.2961(\lg\mathrm{Re})^2 - 1.906\lg\mathrm{Re} + 4.282}{\frac{L}{D} + 1.73} \tag{14}$$

Studies show that the constant 1.73 in (14) is a particular value of those terms $\left[-0.6744\left(\frac{L_n}{D}\right)^2 + 0.9442\frac{L_n}{D} + 3.01\left(\frac{L_t}{D}\right)^3 - 14.77\left(\frac{L_t}{D}\right)^2 + 21.65\frac{L_t}{D} - 6.66523\right]$ in the denominator of (8), when L_n/D=1.5, L_t/D=2. So, from (8) and (14), general form of volumetric viscous drag coefficient C_{PV} can be obtained

$$C_{PV} = \frac{-0.02963\frac{L_n}{D} - 0.04001\frac{L_t}{D} - 0.01564(\lg\mathrm{Re})^3 + 0.2961(\lg\mathrm{Re})^2 - 1.9061\lg\mathrm{Re} + 4.4065}{\frac{L}{D} - 0.8993\left(\frac{L_n}{D}\right)^2 + 1.394\frac{L_n}{D} + 3.01\left(\frac{L_t}{D}\right)^3 - 14.77\left(\frac{L_t}{D}\right)^2 + 21.65\frac{L_t}{D} - 6.66} \tag{15}$$

B. Volumetric Frictional Drag Calculation

Also from Fig. 4, the coefficient C_{FV} can be expressed as

$$C_{FV} = k\frac{L}{D} + b \tag{16}$$

where k and b are undetermined parameters related to the L_n/D and L_t/D.

Table II and Table III list parameters k_n, b_n, k_t and b_t at different L_n/D and L_t/D, respectively. The subscripts n and t identify the parameters related to the nose and tail. From Tables II and III, it is observed that both k_n and k_t fluctuate around 0.0014, and b_n and b_t go up and down around 0.0025. That is to say, L_n/D and L_t/D have a little effect on C_{FV} and can be dismissed.

TABLE II THE VALUES OF k, b WITH DIFFERENT L_n/D
($\mathrm{Re} = 1.525\times10^6$, $L = 3\mathrm{m}$, $L_t/D = 2$, $v = 0.5\mathrm{m/s}$, $n_n = 2$, $n_t = 2$)

L_n/D	k_n	b_n
0.75	0.001396	0.02488
1	0.001397	0.0251
1.25	0.001418	0.0251
1.5	0.001395	0.02544
1.75	0.001368	0.02588
2	0.001353	0.02614

TABLE III THE VALUES OF k , b WITH DIFFERENT L_t / D

($Re = 1.525\times10^6$, $L = 3m$, $L_n / D = 1.5$, $v = 0.5m/s$, $n_n = 2$, $n_t = 2$)

L_t/D	k_t	b_t
1	0.001411	0.02549
1.25	0.001413	0.02546
1.5	0.001418	0.0254
1.75	0.001406	0.02546
2	0.001395	0.02544
2.25	0.001395	0.02551

So, substituting $k = 0.0014$ and $b = 0.0025$ into (17), we have the empirical formula of C_{FV} with L/D

$$C_{FV} = 0.0013\frac{L}{D} + 0.025 \qquad (17)$$

Also from Fig. 5, the mathematic relationship between C_{FV} and Re in different L/D can be expressed as

$$C_{FV} = \frac{r}{\lg Re + s} \qquad (18)$$

where r and s are undetermined parameters related to the L/D. Table IV shows the values of r and s at different L/D.

TABLE IV THE VALUES OF R, S WITH DIFFERENT L/D

($L = 3m$, $L_n / D = 1.5$, $L_t / D = 2$, $n_n = 2$, $n_t = 2$)

L/D	r	s
4	0.06833	-3.922
5	0.07180	-3.920
6	0.07588	-3.919
7	0.08005	-3.883
8	0.08357	-3.856
9	0.08619	-3.886
10	0.09142	-3.838
11	0.09350	-3.860
12	0.09497	-3.910

From Table IV, it can be found that s fluctuates around -3.88 and r go up linearly with the increase of L/D. The relationship between r and L/D can be expressed

$$r = 0.003431\frac{L}{D} + 0.05529 \qquad (19)$$

Substituting (19) and $s = -3.88$ into (18), we obtain the relationship among C_{FV}, lgRe and L/D

$$C_{FV} = \frac{0.003431\frac{L}{D} + 0.05529}{\lg Re - 3.88} \qquad (20)$$

In fact, (17) is a special form of (20) when $Re = 1.525\times10^6$. So (20) is the general form of the volumetric frictional drag coefficient C_{FV}.

C. Model verification

To verify the established empirical formulae (15) and (20) of the drag coefficients, values of C_{PV} and C_{FV} obtained from (15) and (20) are compared with those obtained from CFD method. Accuracy of CFD method has been evaluated in literature [13]. Five sets of design parameters, which are listed in Table V, are used to calculate the corresponding drag coefficients. Table VI and Table VII illustrate the corresponding drag coefficients obtained from the empirical formulae and the CFD method. Errors between the formulae and the CFD simulation are no more than ±10%. It is deemed that the formulae of the drag coefficients are credible.

TABLE V SHAPE PARAMETERS OF AUV ($v = 0.5m/s$)

Test No.	D(mm)	L/D	L_n/D	L_t/D	Re ($\times10^6$)
1	400	7.5	1.3	1.7	1.525
2	240	10	1.5	2	1.220
3	450	8.89	1.11	2.22	2.034
4	400	5.5	1.375	1.125	1.119
5	220	10.45	1.364	1.723	1.169

TABLE VI COMPARISON OF C_{PV} FROM FORMULAS AND CFD

Test No.	*Formula*	*CFD*	*Error*
1	0.013694	0.013887	-1.41%
2	0.010515	0.010395	1.15%
3	0.010919	0.011436	-4.52%
4	0.018165	0.018377	-1.15%
5	0.010814	0.010203	5.99%

TABLE VI COMPARISON OF C_{FV} FROM FORMULAS AND CFD

Test No.	*Formula*	*CFD*	*Error*
1	0.035218	0.036079	-2.39%
2	0.040710	0.042236	-3.61%
3	0.035400	0.035568	-0. 47%
4	0.034191	0.033410	2.34%
5	0.041771	0.041587	0.44%

V. CONCLUSIONS

Hydrodynamic shape genealogy of AUVs was brought forward to make a systematic research on efficient design for the hydrodynamic shape of AUVs with minimum hydrodynamic drag. It is proved that the proposed hydrodynamic shape genealogy is helpful to clarify relationship among the drag coefficients and shape parameters of AUVs.

For the teardrop–shaped AUVs, the shape parameters of L_n/D, L_t/D and L/D and Reynolds number have great effect on volumetric drag coefficients C_{DV}, C_{PV}, and C_{FV}, while profiles of the nose and tail have little influence on them. Actually, effects of those shape parameters and Re on C_{PV}, C_{FV} and C_{DV} are complex, and there is coupling among the parameters.

The empirical mathematical model of volumetric drag coefficient with the shape parameters L_n/D, L_t/D, L/D and Re are constructed and verified.

The present work provides guidance for rapid design of the AUVs hull shape. More detailed discussions about the hydrodynamic shape genealogy will be included in the future research work.

Acknowledgment

The authors are grateful to National Natural Science Foundation of China (granted No. 51675372), National science and technology major projects of China (granted No. 2016ZX05057-005) and National Key Research and Development Program of China (granted No. 2016YFC0301101) for providing support for the investigation. They also would like to express their sincere thanks to L. Ma for her help to revise the grammar.

References

[1] Q. Chen, "Unmanned underwater vehicle". Beijing, National Defence Industry Press, 2014, pp. 47–49.

[2] N. M. Nouri, M. Zeinali, Y. Jahangardy, "AUV hull shape design based on desired pressure distribution," Journal of Marine Science and Technology, vol. 21,pp. 203–215, 2016.

[3] Paster D, "Importance of hydrodynamic considerations for underwater vehicle design", IEEE Oceans, pp. 1413-1422, 1986.

[4] X. S. Jiang，X. S. Feng and L. T. Wang, "Underwater robot", Shenyang: Liaoning Science and Technology Press, pp. 257-263, 2000.

[5] Khairul Alam, Tapabrata Ray, Sreenatha G. Anavatti. "A brief taxonomy of Autonomous underwater Vehicle design literature", J Ocean Engineering, vol. 88, pp. 627-630, 2014.05.

[6] Ikuo Yamamoto. "Research on next autonomous underwater vehicle for longer distance cruising", J. IFAC-PapersOnLine, vol. 48, pp. 173-176, 2015.

[7] Khairul Alam, Tapabrata Ray, Sreenatha G. Anavatti. "Design and construction of an autonomous underwater vehicle", J. Neurocomputing. Vol. 142, pp. 16-29, 2014.05.

[8] Zhiwei Li, Weicheng Cui. "Overview on the hydrodynamic performance of underwater gliders", J. Journal of ship mechanics, vol. 16, pp. 829-836, 2012.7.

[9] S. Z. Chen. "Research on the pedigree of British architectural technology aesthetics", Ph.D. dissertation, Harbin TechnicalUniversity, Heilongjiang, 2013, in Chinese.

[10] Li He, Ling Li. "A new assumption of hierachical classification of Sino-Tibetan languages", J, China Tibetology, vol. 2, pp: 188-191, 2015.

[11] Lewis, E. V. (ed.). Principle of naval architecture, 2nd ed, Society of Naval Architects and Marine Engineers, Jersey city, pp. 18-19 ,1988.

[12] Song Fangxi, Zhang Lianhong, Wu Zhiliang, And Wang Leping. "On resistance calculation for autonomous underwater vehicles", Advanced material Research, vol.189-193, pp. 1745-1748, 2011.

[13] Pareecha Rattanasiri, PhilipA. Wilson, Alexander B. Phillips. "Numerical investigation of a fleet of towed AUVs", J. Ocean Engineering, vol. 80, pp. 25-35, 2014.